CORROSION SCIENCE AND TECHNOLOGY, Vol.23, No.3(2024), pp.221~227 pISSN 1598-6462 / eISSN 2288-6524
[Research Paper] DOI: https://doi.org/10.14773/cst.2024.23.3.221

Structure of Surface Oxide Formed on Zinc-Coated Steel Sheet During Hot Stamping

Shota Hayashida†, Takuya Mitsunobu, and Hiroshi Takebayashi

Steel Research Laboratories, Nippon Steel Corporation, Chiba 293-8511, Japan
(Received February 07, 2024; Revised May 13, 2024; Accepted May 25, 2024)

During hot stamping of hot-dip zinc-coated steel sheets such as hot-dip galvanized steel sheets and hot-dip galvannealed steel sheets, an oxide mainly composed of ZnO is formed on the sheet surface. However, excessive formation of ZnO can lead to a decrease in the amount of metal Zn in the coating layer, decreasing the corrosion resistance of hot-stamped members. Therefore, it is important to suppress excessive formation of ZnO. While the formation of Al oxides and Mn oxides along with ZnO layer during the hot stamping of hot-dip zinc-coated steel sheets can affect ZnO formation, crystal structures of such oxides have not been elucidated clearly. Thus, this study aimed to analyze structures of oxides formed during hot stamping of hot-dip galvannealed steel sheets using transmission electron microscopy. Results indicated the formation of an oxide layer comprising $ZnAl_2O_4$ at the interface between ZnO and the coating layer with Mn_3O_4 at the outermost of an oxide layer.

Keywords: *Hot-dip galvannealed steel sheets, Hot stamping, Oxidation, ZnO*

1. Introduction

In recent years, there has been an increasing demand for strengthening automobile parts to improve the collision safety of automobiles and reduce fuel consumption by reducing the weight of automobile bodies [1]. Hot stamping [2,3], widely used to manufacture high-strength members, involves heating a steel sheet to the austenitization temperature (approximately 900 ºC) and die quenching by water cooled forming dies to obtain a martensite microstructure. Hot stamping allows the manufacture of high-strength parts with excellent shape retention by suppressing spring-back behavior, generated when manufacturing high-strength parts using cold-press methods [4]. The hot-stamped parts which tensile strength is 1.5 GPa and 1.8 GPa have already been used in practical applications; in addition, with the development of even higher-strength parts underway, hot-stamping is expected to become an in-demand method in the future [5-7].

When using uncoated steel sheets for hot stamping, iron oxide scale is formed on the hot-stamped members surface after hot stamping. This scale affects the weldability of hot-stamped parts; thus, descaling process, such as shot blasting, are generally required [8]. Therefore, coated steel sheets are widely used for hot stamping to suppress the formation of such iron oxide scale. Currently, hot-dip galvanized steel sheets [9], hot-dip galvannealed steel sheets [10] (these will henceforth be collectively referred to as "hot-dip zinc-coated steel sheets" in this paper), and Al–Si–coated steel sheets [11] are used in practical applications as these coated steel sheets enable both the suppression of iron oxide scale formation and improvement of corrosion resistance of the hot-stamped parts [12,13].

In coated steel sheets, both the coating layer and iron substrate undergo alloying reactions during hot stamping, and the surface of the coating layer is oxidized, resulting in significant changes in the coating structure [9,10,14]. Before hot stamping, the coating layer of the hot-dip zinc-coated steel sheets mainly comprises the η-Zn, ζ-$FeZn_{13}$, and δ-$FeZn_7$ phases. However, after hot stamping, the composition changes into phases with higher Fe content, such as the Γ-Fe_3Zn_{10} phase or the α-Fe phase consisting of Zn in solid solution (henceforth, "α-(Fe, Zn) phase") [15]. In addition, an oxide layer, mainly composed of ZnO, with a thickness of several μm, forms on the surface of the coating layer [16-18]. The Γ-Fe_3Zn_{10} phase and α-(Fe, Zn) phase are metallic phases that contain Zn and

†Corresponding author: hayashida.za5.shohta@jp.nipponsteel.com

contribute to the improvement of the corrosion resistance in the hot-stamped parts [14]. However, excessive ZnO formation will decrease the amount of metal Zn in the coating layer, decreasing the corrosion resistance of the hot-stamped member. Therefore, it is important to understand the ZnO formation behavior to suppress the excess formation of ZnO.

While ZnO is the main oxide formed during the hot stamping of hot-dip zinc-coated steel sheets, Al and Mn oxides have also been reported to be formed along with ZnO [16-18]. Al oxides, derived from the Al added in small amounts to the zinc-coating layer, are formed at the interface between ZnO and the coating layer, with a thickness of several hundreds of nanometers. Mn oxides, derived from the Mn in the steel substrate, form within the ZnO layer. These Al and Mn oxides can affect the ZnO formation rate. Lee *et al.* [16] and Autengruber *et al.* [17] suggested that the Al oxide formed at the interface between ZnO and the coating layer during the early stage of hot stamping suppresses subsequent ZnO formation. While the effect of Mn oxides on ZnO formation is unclear, they may suppress ZnO formation in a manner similar to that of Al oxides.

However, the crystal structures of these oxides have not yet been elucidated clearly. Al oxides include γ-Al_2O_3 (tetragonal system), α-Al_2O_3 (cubic system), and θ-Al_2O_3 (monoclinic system); however, it is unclear which structure of Al oxide is formed during hot stamping. Similarly, Mn oxides include α-Mn_2O_3 (cubic system), γ-Mn_2O_3 (tetragonal system), and Mn_3O_4 (tetragonal system). Generally, changes in the crystal structures of such oxides affect the diffusion coefficients of substances within the oxides, which can impact the barrier effects affecting ZnO formation. Therefore, it is important to clarify the crystal structures of these oxides to elucidate the effects of Al and Mn oxides on ZnO formation. Thus, in this study, it was analyzed the structures of the oxides formed during the hot stamping of hot-dip galvannealed steel sheets using transmission electron microscopy (TEM).

2. Experimental Methods

2.1. Specimen

Cold-rolled steel sheets (thickness 1.6 mm), with their chemical composition presented in Table 1, were used as the substrates, with a laboratory hot-dip coating simulator used to prepare the hot-dip galvannealed steel specimens. The steel sheets was first annealed at 800 ºC for 60 s in an N_2–4 vol.%-H_2 gas atmosphere with a dew point of −40 ºC and then cooled to 450 ºC and dipped in a Zn–0.14%-Al bath for 3 s for hot-dip coating. Next, an alloying heat treatment was conducted at 520 ºC for 10 s to allow the Fe of the steel substrate to react with the coating layer, with the coated steel sheets cooled from 520 ºC to 150 ºC at a rate of approximately 8 ºC/s by blowing N_2 gas.

Table 1. Chemical composition of steel (mass%)

C	Si	Mn	Cr	Fe
0.2	0.01	1.2	0.2	Bal.

Table 2. Chemical composition of coating layers (mass%)

Zn	Fe	Al
86.0	13.7	0.3

Table 2 presents the chemical composition of the coating layer, measured by immersing the specimen in a 10 vol.% HCl aqueous solution to which 1 vol.% of inhibitor was added to dissolve only the coating layer. High-frequency inductively coupled plasma emission spectrometric analysis was conducted for each element in the aqueous solution after dissolution. In both cases, the amount of Zn deposited on one side of the coating layer was set to approximately 50 g/m^2.

2.2. Simulated heating of hot stamping

The specimens were placed on refractory bricks in an air-heated furnace at a temperature of 900 ºC, heated for various times, and then removed from the furnace and immediately water-cooled. Water cooling was performed to simulate the method of rapid cooling using a cooling mold, as utilized in hot-stamp molding. In this study, clear exfoliation of the coating film and surface oxide film was not observed because of the water-cooling process. Fig. 1 shows an example of the thermal curves during heating, with a K-type thermocouple welded to the surface of the specimen to measure the time required for the specimen to reach a temperature of 900 ºC when placed within a furnace air-heated to 900 ºC. Approximately 140 s were required for the temperature to increase from room temperature to

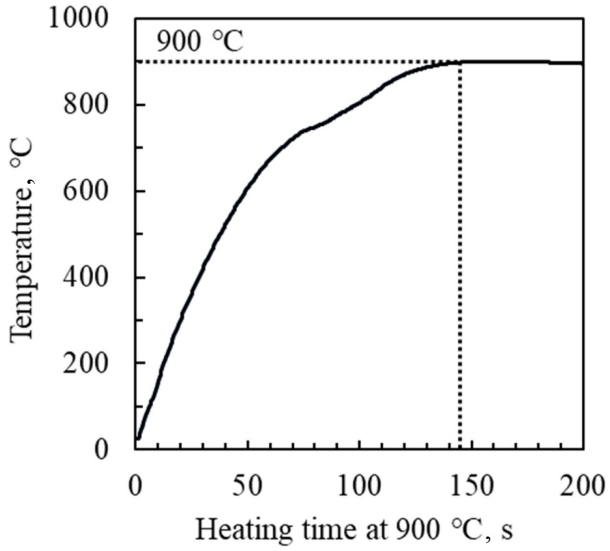

Fig. 1. Temperature curves measured using thermocouples

900 ºC. Generally, in the hot-stamping method, steel sheets are heated to 900 ºC to ensure proper hardening. In this study, the results in Fig. 1 were used as a basis to conduct a heating test that simulated hot stamping by heating the specimen in an air-heated furnace at 900 ºC for 140 s.

2.3. Structural analysis of coating layer and oxide

The constituent phases of the coating layer and oxide film before and after hot stamping were identified through X-ray diffraction (XRD) (RINT-TTR III, Rigaku Corporation). The X-ray tube was irradiated with Cu–Kα radiation, with an acceleration voltage of 40 kV, a current of 150 mA, and a 2θ scanning range of 30–50º.

A scanning electron microscope (SEM) (JSM-7000F, JEOL Ltd.) was used to observe the cross-sections of the coating layer and oxide film before and after hot stamping. The specimens for observation were embedded in resin, mechanically polished using emery paper (#80–#2000), and finally, diamond polished to obtain a mirror finish. The observation mode was set to obtain a backscattered electron image, with an acceleration voltage of 15 kV.

As thin oxides were formed during the hot stamping of hot-dip zinc-coated steel sheets, the cross-sections of the oxide films after hot stamping were observed using TEM (JEM-2100F, JEOL Ltd.). After carbon was deposited on the specimen surface to protect the surface, a thin-section specimen was obtained by focused-ion-beam processing. A bright-field image was captured at an acceleration voltage of 200 kV, and energy-dispersive X-ray spectroscopy (EDS) was conducted. In addition, selected area electron diffraction (SAED) images were captured to identify the constituent phases.

3. Results

3.1. Changes in coating layer due to hot stamping and oxide formation

Fig. 2 and 3 show the XRD profile and backscattered electron images, respectively, of the coating layer cross-section before and after hot stamping. In the XRD profile, mainly the δ-$FeZn_7$ phase can be detected before hot stamping, whereas the Γ-Fe_3Zn_{10} phase, α-Fe phase, and ZnO (hexagonal system) are detected after hot stamping. As observed from the backscattered electron image of the cross-section of the coating layer, a coating layer composed mainly of the δ-$FeZn_7$ phase, with a thickness of approximately 7.6 μm, is formed before hot stamping. After hot stamping, the coating layer thickness increases to approximately 13.5 μm and contrasting bright (top) and dark (bottom) phases and surface oxides are formed. This coating layer is similar to the coating layer formed after

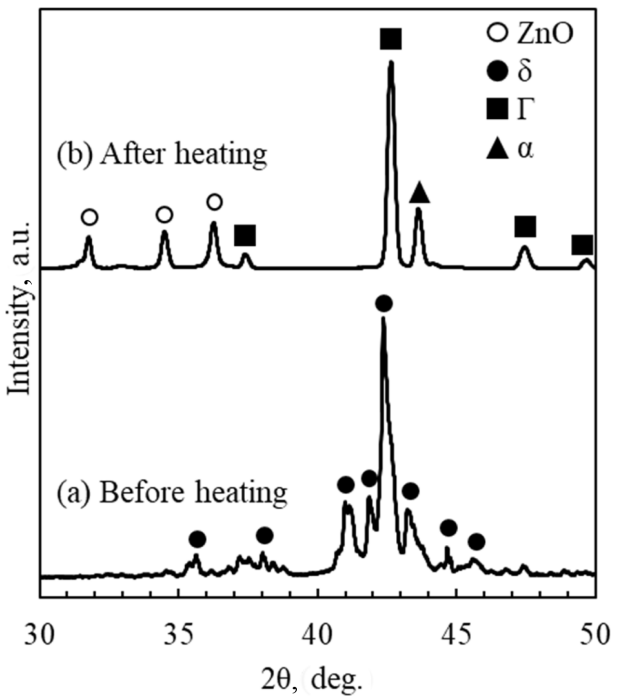

Fig. 2. XRD spectra of specimen: (a) before heating and (b) after heating

the hot stamping of general hot-dip zinc-coated steel sheets [15], with the contrasting bright (top) and dark (bottom) phases and surface oxides considered to mainly comprise the Γ-Fe_3Zn_{10} phase, the α-(Fe, Zn) phase, and ZnO.

3.2. TEM analysis of oxides formed during hot stamping

Fig. 4 and 5 show the bright-field images of the oxide cross-section after hot stamping, EDS element distribution maps, and the phase identification results using the SAED

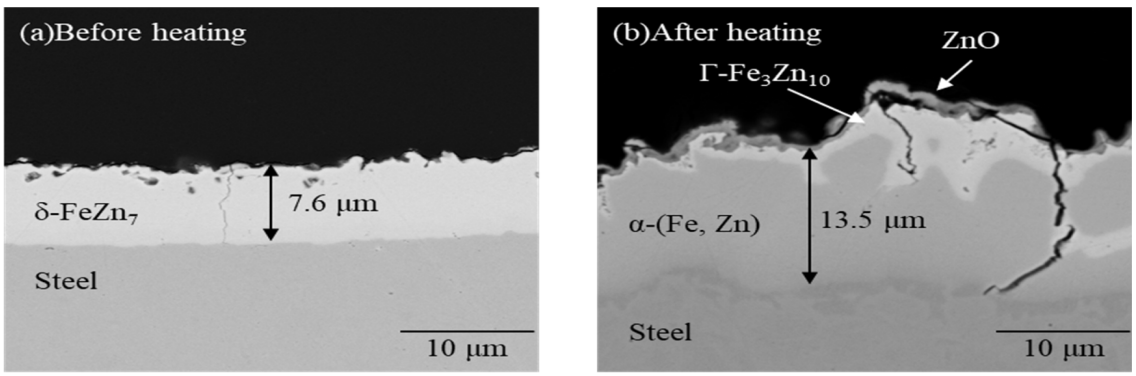

Fig. 3. Cross-sectional SEM images of specimen: (a) before heating and (b) after heating

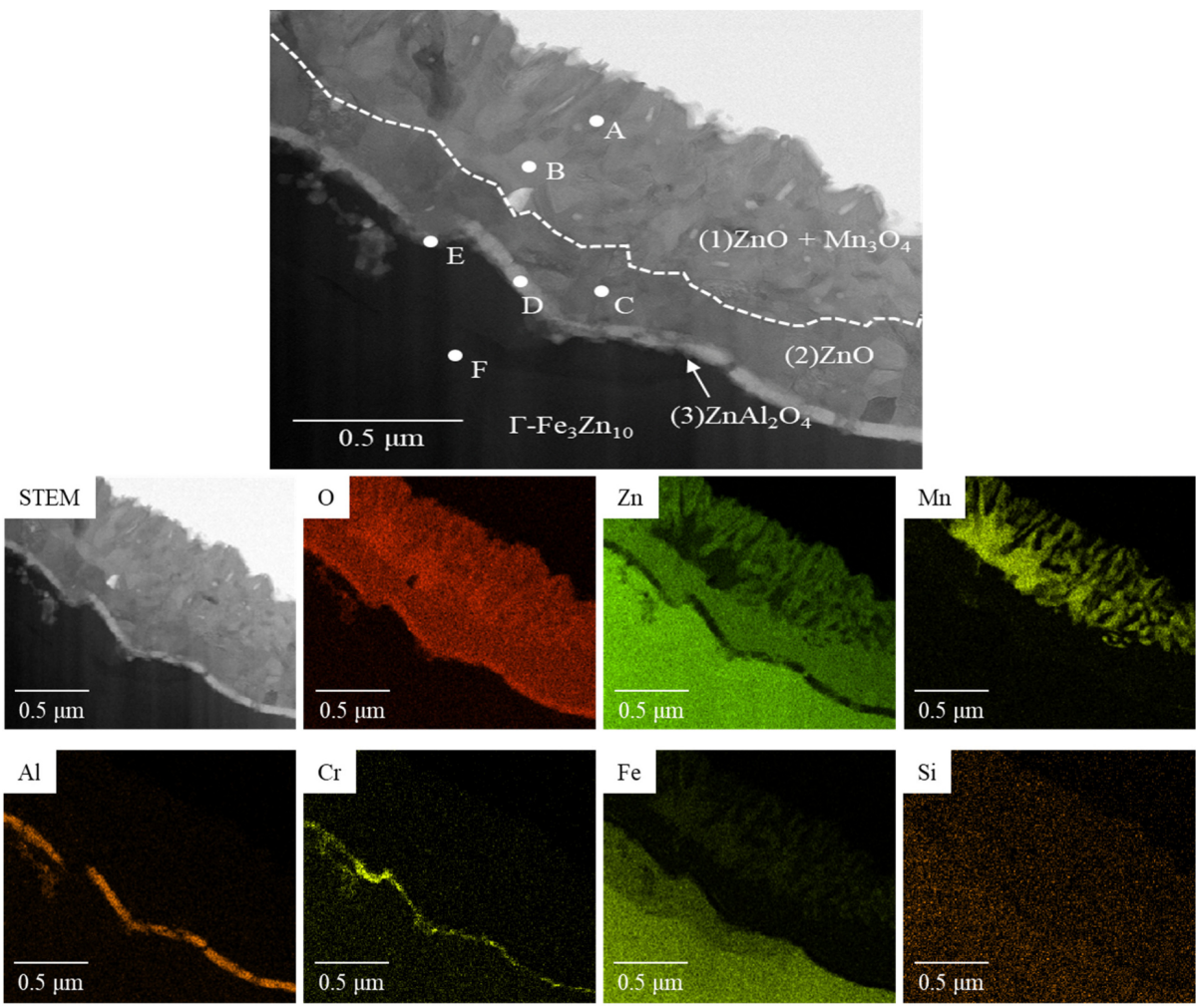

Fig. 4. TEM image and EDS maps of specimen after heating

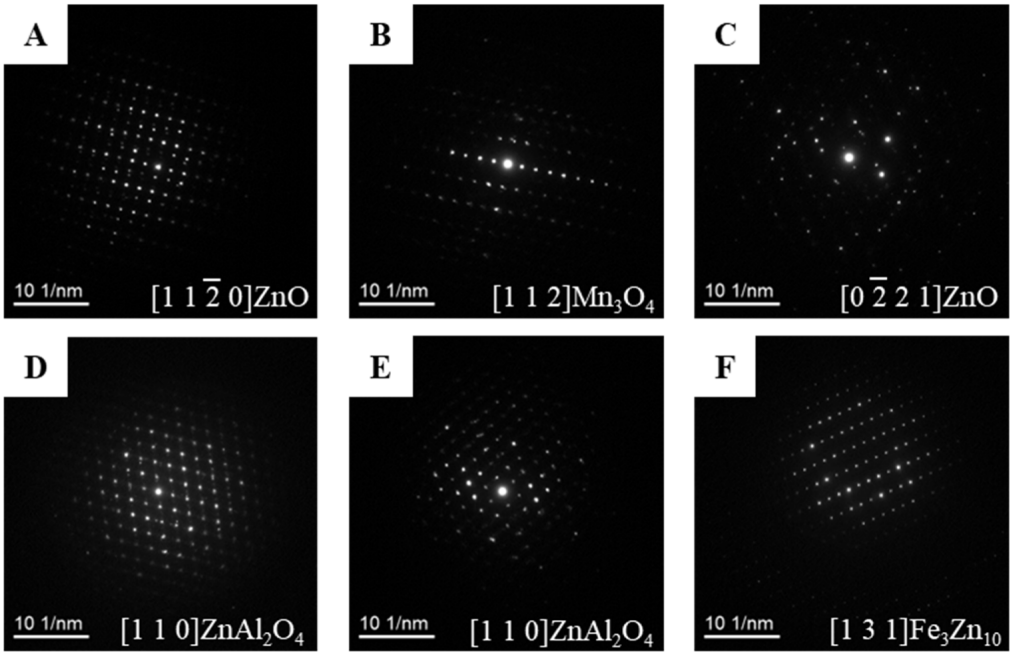

Fig. 5. SAED images of specimen after heating

Table 3. TEM-EDS analysis measured from area A–F in Fig. 4

Area	Oxid layer	Chemical composition (at. %)							Phase	System
		O	Al	Si	Cr	Mn	Fe	Zn		
A	(1)	37.0	N.D.	0.3	0.2	5.2	1.6	55.4	ZnO	Hexagonal
B	(1)	50.7	N.D.	0.2	N.D.	26.9	1.6	20.4	Mn_3O_4	Cubic
C	(2)	40.5	0.1	N.D.	N.D.	2.2	0.9	56.3	ZnO	Hexagonal
D	(3)	69.1	20.2	0.2	0.6	0.3	0.2	9.5	$ZnAl_2O_4$	Cubic
E	(3)	59.3	15.3	0.4	3.8	0.7	0.4	20.0	$ZnAl_2O_4$	Cubic
F	-	3.3	0.2	0.3	0.4	N.D.	19.2	76.0	Fe_3Zn_{10}	Cubic

image at points A–F. Table 3 shows the results of the EDS composition analysis and identified phases. The element distribution maps suggest that the oxide contains Al, Mn, and Cr, in addition to Zn. The oxide has a three-layer structure; from the surface to the inside, it is composed of (1) an oxide layer of approximately 0.5-μm-thick Zn as well as Mn and O, (2) an oxide layer of approximately 0.3-μm-thick Zn and O, and (3) an oxide layer of approximately 30-nm-thick Zn, Al, Cr, and O. Based on the SAED images, the structures of the oxide phases constituting layers (1), (2), and (3) were identified as hexagonal ZnO and cubic Mn_3O_4, hexagonal ZnO, and cubic $ZnAl_2O_4$, respectively.

4. Discussion

Al oxides and Mn oxides are formed along with ZnO in hot-dip zinc-coated steel sheets during hot stamping; however, their crystal structures have remained unclear. Through a TEM analysis, it is identified that the Al and Mn oxides are in the form of cubic $ZnAl_2O_4$ and cubic Mn_3O_4, respectively. Below, we discuss the factors affecting the formation of $ZnAl_2O_4$ and Mn_3O_4.

The bright-field image of the oxide cross-section in Fig. 4 shows that $ZnAl_2O_4$ was formed adjacent to ZnO. Fig. 6 presents the phase diagram of the pseudo-binary ZnO–Al_2O_3 system [19], with Al_2O_3 (C), ZnO (Z), $ZnAl_2O_4$ (S), and the liquid phase (L) shown in this phase diagram.

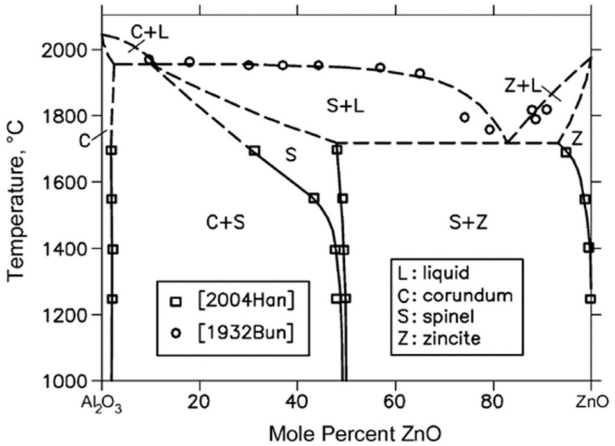

Fig. 6. Al_2O_3-ZnO pseudo-binary section. Liquid (L), corundum (C), spinel (S), and zincite (Z) are indicated in the diagram

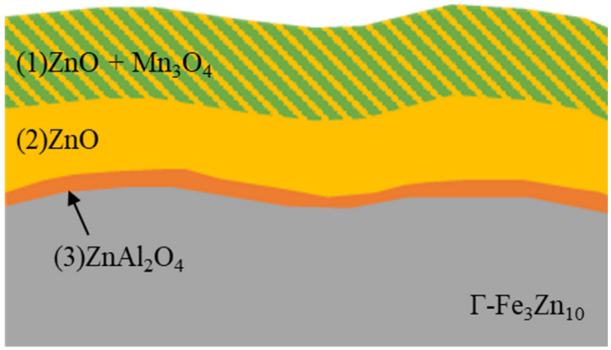

Fig. 7. Schematic of oxide layer formed on specimen after heating

This phase diagram shows that ZnO and $ZnAl_2O_4$ are in thermodynamic equilibrium. Therefore, $ZnAl_2O_4$ can be assumed to have been formed in hot-dip zinc-coated steel sheets because of the oxidation of Zn along with that of Al. During hot stamping, the oxidation of Al, which is easily oxidized [20], occurs first, following which the oxidation of Zn occurs and ZnO is formed at the outside of the Al oxide layer after the complete oxidation of metallic Al in the coating layer [16,17]. Therefore, Al_2O_3 may be formed in the initial heating stage before changing to $ZnAl_2O_4$ as Zn oxidation proceeds; however, this process needs further investigation, which will be done in future studies.

Mn oxides include α-Mn_2O_3 (cubic system), γ-Mn_2O_3 (tetragonal system), and Mn_3O_4 (tetragonal system), from which Mn_3O_4 is formed. Mn_3O_4 is formed adjacent to ZnO and contains approximately 20 at.% Zn, based on the EDS analysis results. In Mn_2O_3, all Mn ions in the oxide are trivalent, whereas, in Mn_3O_4, divalent and trivalent ions exist in a ratio of 1:2. The Mn oxide formed here contains Zn; the Zn ion tends to be divalent. Therefore, Mn_3O_4 may be stabilized by replacing a part of the Mn^{2+} in Mn_3O_4 with Zn^{2+}. In reality, $ZnMn_2O_4$ is recognized as an oxide where all Mn^{2+} ions are replaced with Zn^{2+} ions. Mn_3O_4 is formed at the outside of ZnO layer. As shown in Table 3, metallic Mn is not detected in the coating layer after heating up to 900 ºC, suggesting that most of the Mn, derived from the steel substrate, is oxidized in the heating-up period. Mn is more easily oxidized than Zn [20]. Therefore, ZnO may be formed underside of Mn_3O_4 due to the inward diffusion of oxygen through the Mn_3O_4 formed in the early stage of heating, but the details require further investigation.

Based on the above results, a schematic diagram of the oxides formed during the hot stamping of hot-dip galvannealed steel sheets is shown in Fig. 7. The three-layer structure of the oxide, from the surface to the inside, comprises (1) an oxide layer of ZnO and Mn_3O_4, (2) an oxide layer of ZnO, and (3) an oxide layer of $ZnAl_2O_4$. Understanding the ZnO formation behavior during the hot stamping of hot-dip zinc-coated steel sheets requires using diffusion coefficients of the Zn and O ions in $ZnAl_2O_4$ and Mn_3O_4 for estimating the barrier effects of these oxides on ZnO formation.

5. Conclusion

We used TEM to analyze the structures of the oxides formed during the hot stamping of hot-dip galvannealed steel sheets. The results showed that the oxide formed on the coating layer consisted of Γ-Fe_3Zn_{10} phase had a three-layer structure comprising an oxide layer of hexagonal ZnO and cubic Mn_3O_4 at the outermost surface, followed by an oxide layer of hexagonal ZnO, an oxide layer of cubic $ZnAl_2O_4$ at undermost layer.

References

1. H. Karbasian and A. E. Tekkaya, A review on hot stamping, *Journal of Materials Processing Technology,* **210**, 2103 (2010). Doi: https://doi.org/10.1016/j.jmatpro-

tec.2010.07.019
2. M. Maikranz-Valentin, U. Weidig, U. Schoof, H. H. Becker, and K. Steinhoff, Components with Optimised Properties due to Advanced Thermo-mechanical Process Strategies in Hot Sheet Metal Forming, *Steel Research International*, **79**, 92 (2008). Doi: https://doi.org/10.1002/srin.200806322
3. N. Kojima, *Journal of the Japan Society for Technology of Plasticity*, **46**, 595 (2005).
4. K. Kusumi, S. Yamamoto, T. Takeshita, S. Nakamura, M. Abe, and M. Suehiro, *Proc. The 149th ISIJ Meeting*, p. 556, The Iron and Steel Institute of Japan, Yokohama University, Yokohama (2005).
5. T. Suzuki, T. Niinomi, K. Nakashima, T. Nishibata, and N. Kojima, *Proc. The 155th ISIJ Meeting*, p. 598, The Iron and Steel Institute of Japan, Musashi Institute of Technology, Setagaya (2008).
6. K. Hikida, T. Nishibata, H. Kikuchi, T. Suzuki, and N. Nakayama, Development of TS1800MPa, Grade Hot Stamping Steel Sheet, *Materia Japan*, **52**, 68 (2013). Doi: https://doi.org/10.2320/materia.52.68
7. K. Mori, P. Bariani, B.-A. Behrens, A. Brosius, S. Bruschi, T. Maeno, M. Merklein, and J. Yanagimoto, Hot stamping of ultra-high strength steel parts, *CIRP Annals*, **66**, 755 (2017). Doi: https://doi.org/10.1016/j.cirp.2017.05.007
8. U. Paar, H. Becker, and M. Alsmann, *Proc. 1st International Conference on Hot Sheet Metal Forming of High-Performance Steel*, p. 153, Verlag Wissenschaftliche Scripten, Auerbach (2008).
9. M. Fleischanderl, S. Kolnberger, J. Faderl, G. Landl, A. Raab, and W. Brandstatter, Method for Producing a Hardened Steel Part, *Patents*, US20070256808 (2007). https://patents.google.com/patent/US20070256808
10. Y. Yoshikawa, K. Itami, K. Fukui, T. Toki, S. Sudo, A. Obayashi, and M. Ichikawa, Hot press formed product and method for production thereof, *Patents*, EP1630244 (2009). https://patents.google.com/patent/EP1630244B1/en?oq=EP1630244
11. P. Drillet, D. Spehner, and R. Kefferstein, Coated steel strips, methods of making the same, methods of using the same, stamping blanks prepared from the same, stamped products prepared from the same, and articles of manufacture which contain such a stamped product, *Patents*, WO2008053273 (2008). https://patentscope.wipo.int/search/en/detail.jsf?docId=WO2008053273
12. L. Dosdat, J. Petitjean, T. Vietoris, and O. Clauzeau, Corrosion Resistance of Different Metallic Coatings on Press Hardened Steels for Automotive, *Steel Research International*, **82**, 726 (2011). Doi: https://doi.org/10.1002/srin.201000291
13. R. Autengruber, G. Luckeneder, and A.W. Hassel, Corrosion of press-hardened galvanized steel, *Corrosion Science*, **63**, 12 (2012). Doi: https://doi.org/10.1016/j.corsci.2012.04.048
14. D. W. Fan, H. S. Kim, J. K. Oh, K. G. Chin, and B. C. D. Cooman, Coating Degradation in Hot Press Forming, *ISIJ International*, **50**, 561 (2010). Doi: https://doi.org/10.2355/isijinternational.50.561
15. A. Sengoku, H. Takebayashi, N. Okamoto, and H. Inui, Structural Changes in Galvannealed Coating during Hot-stamping Heating, *Tetsu-to-Hagané*, **104**, 331 (2018). Doi: https://doi.org/10.2355/tetsutohagane.TETSU-2017-100
16. C. W. Lee, W. S. Choi, Y. R. Cho, and B. C. D. Cooman, Surface Oxide Formation during Rapid Heating of Zn-coated Press Hardening Steel, *ISIJ International*, **54**, 2364 (2014). Doi: https://doi.org/10.2355/isijinternational.54.2364
17. R. Autengruber, G. Luckeneder, A. S. Kolnberger, J. Faderl, and A. W. Hassel, Surface and Coating Analysis of Press-Hardened Hot-Dip Galvanized Steel Sheet, *Steel Research International*, **83**, 1005 (2012). Doi: https://doi.org/10.1002/srin.201200068
18. W. Gaderbauer, M. Arndt, T. Truglas, T. Steck, N. Klingner, D. Stifter, J. Faderl, and H. Groiss, Effects of alloying elements on surface oxides of hot-dip galvanized press hardened steel, *Surface and Coatings Technology*, **404**, 126466 (2020). Doi: https://doi.org/10.1016/j.surfcoat.2020.126466
19. R. Hansson, P. C. Hayes, and E. Jak, Experimental study of phase equilibria in the Al-Fe-Zn-O system in air, *Metallurgical and Materials Transactions B*, **35**, 633 (2004). Doi: https://doi.org/10.1007/s11663-004-0004-x
20. M. Shamsuddin, *Physical Chemistry of Metallurgical Processes, Second Edition*, Springer Cham (2021). Doi: https://doi.org/10.1007/978-3-030-58069-8